physica status solidi b
www.pss-b.com

Metastable Changes in the Dark Conductivity of Undoped and Carbon-Doped β-Ga_2O_3

Norbert H. Nickel, Niccolò Mignani, and Jörg Rappich*

Measurements of the electrical dark conductivity σ_D of undoped and carbon-doped β-Ga_2O_3 thin films reveal a metastable increase upon illumination with sub-bandgap light. In the relaxed state, σ_D shows activated behavior for $T > 250$ K with an activation energy of 0.68 and 0.63 eV for undoped and C-doped β-Ga_2O_3, respectively. For $T < 250$ K, σ_D approaches a constant value of $\approx 6 \times 10^{-12}\,\Omega^{-1}\,cm^{-1}$. Illumination with sub-bandgap light results in an increase of the dark conductivity by up to 6 orders of magnitude. This state is metastable and relaxes with time. The data indicate the presence of a broad distribution of localized states in the bandgap. The time and temperature dependence of the relaxation is investigated for doped and undoped samples. The data can be described by a sum of two and three stretched exponential decays for undoped and carbon-doped β-Ga_2O_3, respectively. From the time constants of the decays, the energetic depth of the localized defect states is estimated.

1. Introduction

For some time, β-Ga_2O_3 has been the focus of research for applications comprising high-power devices, solar-blind photodetectors, and transparent conducting oxides.[1–3] Several applications such as MOSFETs with breakdown voltages of more than 750 V have been demonstrated.[4] The breakdown voltage depends on the defect concentration and is sensitive to controlled doping. However, undoped β-Ga_2O_3 shows n-type conductivity with carrier concentrations of about $2 \times 10^{18}\,cm^{-3}$. Originally, this was attributed to oxygen vacancies.[5] However, ab initio calculations suggest that the origin of n-type conductivity is associated with the incorporation of hydrogen.[6] This is corroborated by recent hydrogen effusion measurements that revealed a hydrogen concentration of about $1 \times 10^{18}\,cm^{-3}$ in as-grown single crystal β-Ga_2O_3.[7]

For devices that rely on the electronic properties of β-Ga_2O_3, it is important to control the carrier concentration. This requires 1) a controllable adjustment of the charge carrier concentration through doping and 2) a low concentration of localized defects. While achieving p-type doping is difficult and only low carrier concentrations are obtained,[8] n-type doping with Si, Sn, and Ge is well established. Furthermore, for n-type doping, the electron concentration can be controlled in the range of 10^{16}–$10^{19}\,cm^{-3}$.[9–11] The latter point, namely the concentration and energetic position of localized defects, depends on growth conditions and impurity concentrations of, for example, trace metals in the precursor materials that are being used. Depending on the nature of the localized defect, they can occur in a broad energy range in the bandgap.[12] Metal trace impurities such as Mg and Fe introduce deep acceptor-like states at about 1.1[13,14] and 0.78 to 0.86 eV below the conduction band,[13,15] respectively. In addition, when β-Ga_2O_3 thin films are deposited by methods that result in polycrystalline samples, grain-boundary defects that may consist of broken and strain bonds will also contribute to the defect distribution in the bandgap.

In this article, the time and temperature dependence of the dark conductivity, σ_D, is investigated for undoped and carbon-doped polycrystalline β-Ga_2O_3. Upon illumination, σ_D increases by up to 6 orders of magnitude at low temperatures. This excited state is metastable and an anneal at elevated temperatures results in a decrease of σ_D to a ground state. The data show that a large concentration of localized defects in the bandgap with a broad energy distribution controls the time and temperature dependence of σ_D.

2. Experimental Details

The specimens investigated in this work were grown by plasma-assisted pulsed laser deposition (PLD). As a light source, a KrF excimer laser emitting at a wavelength of 248 nm was used. The laser was operated with a repetition rate of 10 Hz and the laser pulses had a length of 25 ns. Gallium oxide targets were fabricated by the following steps. Ultrapure Ga_2O_3 powder was pressed to small targets with a pressure of about 110 kg cm^{-2}. In a second step, the targets were annealed for 5 h at 1100 °C in air to obtain ceramic targets. Using the PLD setup, nominally undoped and carbon-doped β-Ga_2O_3 thin films were deposited

N. H. Nickel, N. Mignani, J. Rappich
Nanoscale Solid Liquid Interfaces
Helmholtz-Zentrum Berlin für Materialien und Energie
Schwarzschildstr. 8, 12489 Berlin, Germany
E-mail: nickel@helmholtz-berlin.de

The ORCID identification number(s) for the author(s) of this article can be found under https://doi.org/10.1002/pssb.202400471.

DOI: 10.1002/pssb.202400471

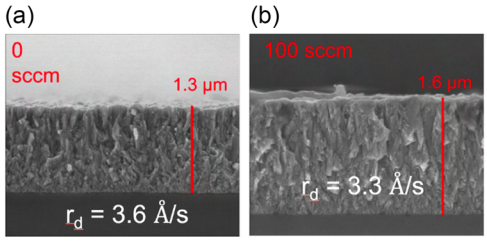

Figure 1. Cross-sectional SEM micrographs of β-Ga_2O_3 thin films deposited by PLD. The deposition temperature amounted to $T = 600\,°C$. The sample depicted in a) is nominally undoped and the sample shown in b) was grown with a CO_2 flow rate of 100 sccm. The average grain size is about 100 nm.

on *c*-axis oriented sapphire substrates. Contamination of the samples with aluminum from the sapphire substrates was avoided by depositing a 5 nm-thick MgO layer prior to the growth of β-Ga_2O_3. Carbon doping was achieved by adding a constant flow of CO_2 to the deposition chamber. The doping gas was ionized in an optically isolated remote microwave plasma. The samples were grown at a substrate temperature of $T = 600\,°C$. The resulting carbon concentration in the samples was measured using secondary ion mass spectrometry (SIMS). Information on the microscopic structure was obtained from scanning electron microscopy (SEM, **Figure 1**) and from micro-Rama backscattering measurements. For the latter, an excitation wavelength of $\lambda = 633\,nm$ was used. To perform electrical measurements, coplanar ohmic contacts consisting of titanium covered with a gold layer were deposited on top of the β-Ga_2O_3 samples. The contacts yielded linear *I*–*V* curves for voltages of up to ±100 V. Temperature-dependent dark-conductivity measurements were performed with a heating rate of 0.1 K s^{-1}. All electrical measurements were performed in an oil-free vacuum.

3. Results and Discussion

The data presented in this section were obtained from SEM, SIMS, Raman scattering, and conductivity measurements. In Section 2.1, the structural properties of the PLD-grown β-Ga_2O_3 thin films are presented. Then, in Section 2.2, metastable changes of the electrical dark conductivity upon annealing and illumination with sub-bandgap light are discussed. The time and temperature dependence of the relaxation are shown in Section 2.3, and data on the energetic position of localized defect states, deduced from the relaxation time constants, are given in Section 2.4.

3.1. Structural Properties

Figure 1 shows cross-sectional SEM micrographs of PLD-grown β-Ga_2O_3. The micrographs show that both the undoped (a) and carbon-doped (b) samples are composed of small grains with an average grain size of $\langle x \rangle \approx 100\,nm$. Both samples were deposited with identical parameters except for the flow of CO_2. The deposition rate amounted to $r_d = 3.3$–$3.6\,Å\,s^{-1}$. This shows that the addition of a CO_2 flow of up to l00 sccm had no effect on the overall growth and microscopic structure of the samples.

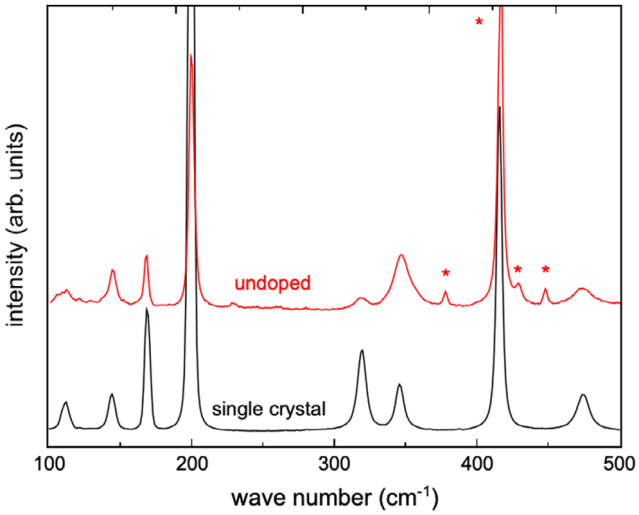

Figure 2. Raman backscattering spectra of single crystal (black curve) and undoped PLD-grown β-Ga_2O_3 (red curve). The measurements were performed with an excitation wavelength of 633 nm. The asterisks indicate phonon modes from the sapphire substrate.

Additional information on the structural properties of the samples was obtained from Raman backscattering measurements. In **Figure 2**, the phonon spectrum of undoped β-Ga_2O_3 (red line) is compared to that of single crystal β-Ga_2O_3 (black line). A close examination of the phonon modes of the polycrystalline thin films shows excellent agreement of the peak positions and their line widths with single crystal β-Ga_2O_3. Note that the additional phonon modes marked with an asterisk originate from the sapphire substrate.

When carbon is used as a dopant in β-Ga_2O_3, the C atom replaces a Ga atom. Since carbon is smaller than gallium, the C atom shifts away from the substitutional Ga site toward the interstitial site. As a consequence, the bonds to the nearest neighbor O atoms decrease. This configuration is known as a DX center.[16] Subsequently, this configuration introduces strain, and it is conceivable that some of the phonon modes are sensitive to it. **Figure 3** shows Raman spectra of C-doped β-Ga_2O_3 in comparison to an undoped specimen. The doped samples were deposited with a CO_2 flow of 40 and 80 sccm. Comparing the phonon spectra of the C-doped specimens to the undoped sample clearly shows that the incorporation of carbon does not affect the phonon frequencies and line widths. Therefore, it can be concluded that the carbon concentration is rather low.

To determine the carbon concentration of the specimens, SIMS measurements were performed. In **Figure 4**, the carbon concentration is shown as a function of the CO_2 flow rate. It is interesting to note that undoped PLD-grown β-Ga_2O_3 (CO_2 flow = 0 sccm) contains a C concentration of $\approx 2.7 \times 10^{18}\,cm^{-3}$. Most likely, this is caused by residual CO_2 in the vacuum chamber. Adding CO_2 to the growth process and ionizing the molecules with a microwave plasma results in a monotonic increase of the carbon concentration up to a flow rate of 40 sccm. For higher flow rates, the C concentration in β-Ga_2O_3 does not change and reaches a value of $\approx 4 \times 10^{19}\,cm^{-3}$.

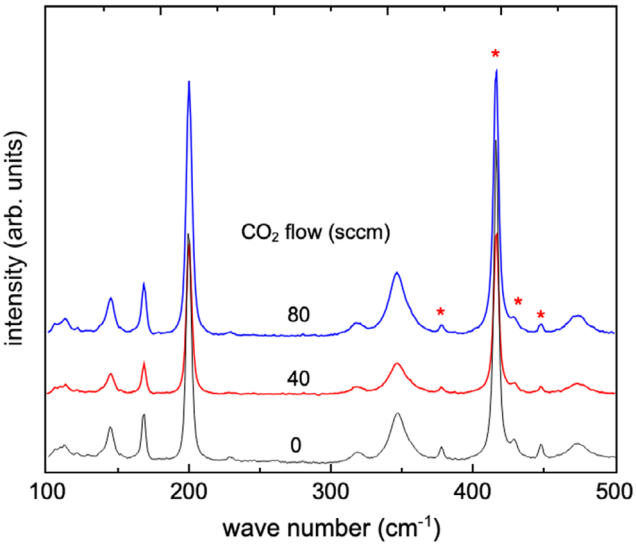

Figure 3. Raman backscattering spectra of undoped and carbon-doped β-Ga_2O_3. Doping was carried out from the gas phase by adding CO_2 and ionizing the molecules in an optically isolated microwave plasma. The asterisks indicate phonon modes from the sapphire substrate.

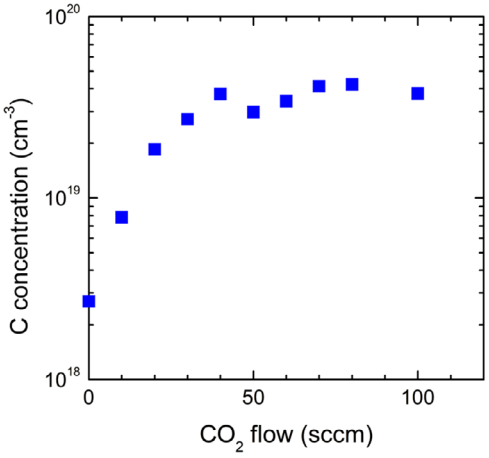

Figure 4. Carbon concentration in β-Ga_2O_3 as a function of the CO_2 gas flow. All samples were deposited at $T = 600$ °C.

3.2. Metastable Changes in the Electrical Conductivity

Figure 5 shows Arrhenius plots of the dark conductivity, σ_D, of undoped β-Ga_2O_3. The inverted triangles represent the relaxed state of β-Ga_2O_3. This state is achieved by annealing the specimen at a temperature of $T = 450$ K for a prolonged time and then cooling it to $T = 78$ K. Subsequently, the dark conductivity is measured while the sample is heated with a heating rate of 0.1 K s^{-1}. The conductivity data show two regimes. At low temperatures ($T < 230$ K), the dark conductivity is almost independent of temperature ($\sigma_D \approx 7 \times 10^{-12}\,\Omega^{-1}\,cm^{-1}$). A close examination of σ_D reveals a very small slope of about 1 meV. Such a behavior is indicative of charge carrier hopping in localized states also known as variable range hopping.[17,18] On the other hand, for $T > 240$ K, activated behavior is observed with an activation energy of $E_A = 0.68$ eV. The temperature dependence of σ_D in the relaxed state A is independent of the heating rate at which the measurement is performed.

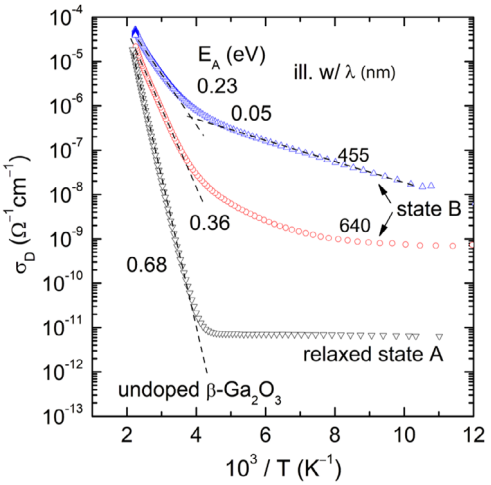

Figure 5. Temperature dependence of the dark conductivity, σ_D, of undoped β-Ga_2O_3. The inverted triangles represent the relaxed state A. The curves shown by the circles and triangles were obtained after the specimen was illuminated with light with a wavelength of $\lambda = 640$ and 455 nm, respectively, at a temperature of $T = 300$ K. The dashed lines are least-squares fits to the data and indicate the activation energies in state A and B.

A pronounced increase in the dark conductivity was observed after prolonged illumination of the specimen with monochromatic light. As light sources, two light-emitting diodes with wavelengths of $\lambda = 455$ and 640 nm were used. It is important to note that both LEDs provide only sub-bandgap light. The illumination was performed at room temperature and continued until the photocurrent was approximately constant. The sample was then cooled to $T = 78$ K and σ_D was measured while the sample was heated with a heating rate of 0.1 K s^{-1}. For $T < 200$ K, an increase of σ_D by more than two orders of magnitude is observed (state B, red circles in Figure 5). As the temperature increases, σ_D exhibits a constant increase and exceeds the dark conductivity of the relaxed state by more than 3 orders of magnitude at $T = 225$ K. The curved behavior of σ_D with temperature is indicative of variable range hopping.[17,18] At high temperatures, σ_D shows activated behavior with a slope of $E_A = 0.36$ eV (red circles in Figure 5).

Illumination of undoped β-Ga_2O_3 with blue light ($\lambda = 455$ nm) results in a further pronounced increase of the dark conductivity in the entire temperature range. At low ($T < 200$ K) and high temperatures ($T > 280$ K) σ_D exhibits activated behavior with a slope of $E_A = 0.05$ and 0.23 eV, respectively (state B, blue triangles in Figure 5).

The same measurements were performed for carbon-doped β-Ga_2O_3. **Figure 6** shows the temperature dependence of σ_D for a sample doped with a C concentration of 3.7×10^{19} cm^{-3}. At low temperatures, σ_D of the relaxed state A is comparable to the dark conductivity of undoped β-Ga_2O_3. For $T > 240$ K, activated behavior is observed with a smaller activation energy of

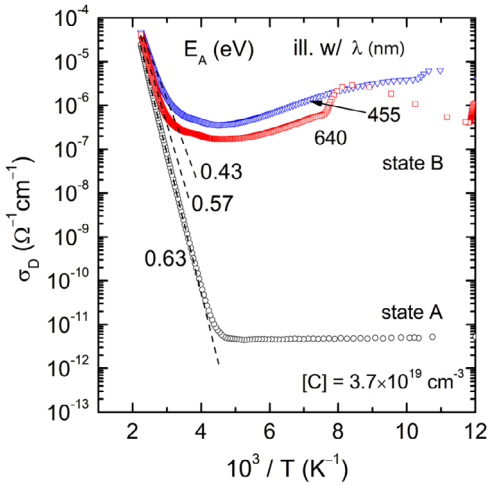

Figure 6. Temperature dependence of the dark conductivity, σ_D, of carbon-doped β-Ga_2O_3. The open circles represent the relaxed state A. The curves shown by the open squares and inverted triangles (state B) were obtained after the specimen was illuminated with light with a wavelength of $\lambda = 640$ and 455 nm, respectively, at a temperature of $T = 300$ K. The dashed lines are least-squares fits to the data and indicate the activation energies in state A and B.

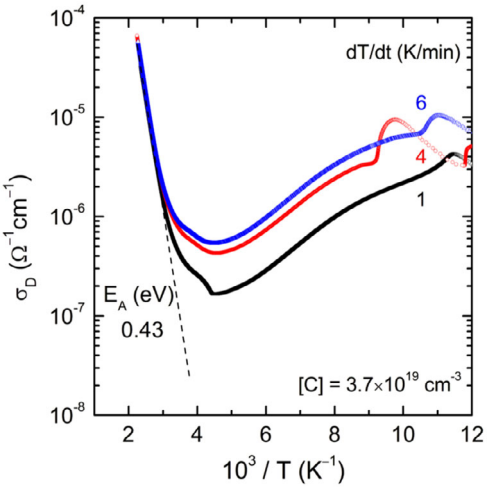

Figure 7. Temperature dependence of the dark conductivity, σ_D, of carbon-doped β-Ga_2O_3 for different heating rates, dT/dt. The carbon concentration amounted to 3.7×10^{19} cm^{-3}.

$E_A = 0.63$ eV. This indicates that C doping introduces localized states somewhat closer to the conduction band.

A more pronounced change is observed in state B. Prolonged illumination with sub-bandgap results in an increase of σ_D for $T < 220$ K by up to 6 orders of magnitude. Moreover, with increasing temperature, σ_D decreases until a minimum is reached at about $T = 225$ K (state B in Figure 6). It is interesting to note that σ_D exhibits a maximum at $T = 110$ K after illumination with light of a wavelength of 640 nm (red squares). This indicates that C doping introduces a large concentration of localized states deep in the bandgap that can enable charge transport controlled by hopping mechanisms at low temperatures. At higher temperatures, activated behavior is observed when the sample is in state B with activation energies of $E_A = 0.57$ and 0.43 eV after illumination with $\lambda = 640$ and 455 nm, respectively.

The changes in the dark conductivity of undoped and C-doped β-Ga_2O_3 are reversible independent of the used wavelength to obtain the enhanced conductivity in state B. Annealing at elevated temperatures results in a decrease of σ_D until the relaxed state A is reached.

In polycrystalline semiconductors, charge transport is governed by potential barriers and localized defects at the grain boundaries. At high temperatures, charge transport is activated and can be described by the Seto model.[19] The deviation from activated behavior at low temperatures could be due to 1) tunneling through the potential barriers, 2) an inhomogeneous character of the samples with respect to the potential barriers and the defect distribution, 3) a distribution of potential barrier heights, or 4) hopping transport in localized defect states. The latter transport process is observed when the mean distance between localized states is larger than the localization length. This requires a moderately high defect concentration close to the Fermi energy. In comparison with other semiconductors such as amorphous silicon, the defect concentration needs to be in the range of about 10^{19} cm^{-3} to observe hopping transport.[20]

The influence of the heating rate at which the dark conductivity was measured is shown in **Figure 7**. Prior to each measurement, the specimen was illuminated with blue light ($\lambda = 455$ nm) until the photocurrent approached a constant value. Then, the sample was cooled to 77 K. Subsequently, σ_D was measured while the sample was heated with the indicated heating rate. With increasing heating rate, the low-temperature branch of σ_D increases by more than a factor of 3. Moreover, for $T < 120$ K, a peak is observed that shifts from 87 to 103 K. The changes of σ_D and the shift of the peak indicate that the charge carriers involved are transported through states in which they are metastable. Through thermal excitation, the charge carriers can leave the localized states and recombine. For $T > 300$ K, the curves merge and show activated behavior with an activation energy of $E_A = 0.43$ eV (see Figure 6 and 7). The data show that charge carrier transport in PLD-grown β-Ga_2O_3 is governed by a complex mechanism due to a distribution of localized defect states in the bandgap.

3.3. Time and Temperature Dependence of the Relaxation

The time and temperature dependence of the relaxation of σ_D from state B to state A was examined. **Figure 8** shows the normalized conductivity transients of undoped β-Ga_2O_3 that were measured at temperatures between 416 and 470 K. The transients show interesting and unexpected behavior that clearly deviates from a simple exponential decay. The decays can be reasonably described by the sum of two stretched exponential functions

$$\frac{\sigma_D}{\sigma_0} = I\exp\left[-\left(\frac{t}{\tau_1}\right)^{\beta_1}\right] + (1-I)\exp\left[-\left(\frac{t}{\tau_2}\right)^{\beta_2}\right] \quad (1)$$

where I and $(1 - I)$ describe the weight of each stretched exponential function, τ_1 and τ_2 are time constants, and β_1 and β_2 are the stretching parameters.

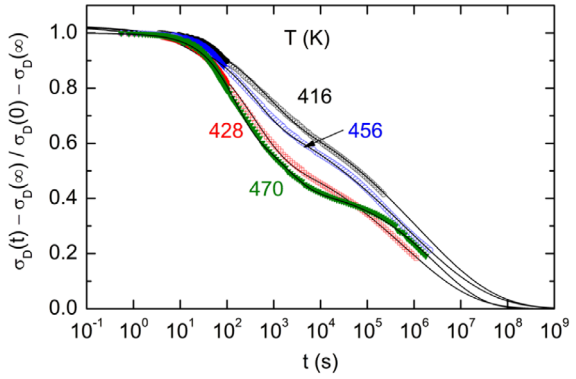

Figure 8. Normalized dark conductivity of undoped β-Ga_2O_3 as a function of time at high temperatures. The data are shown by points and the lines are least-squares fits to the sum of two stretched exponential functions.

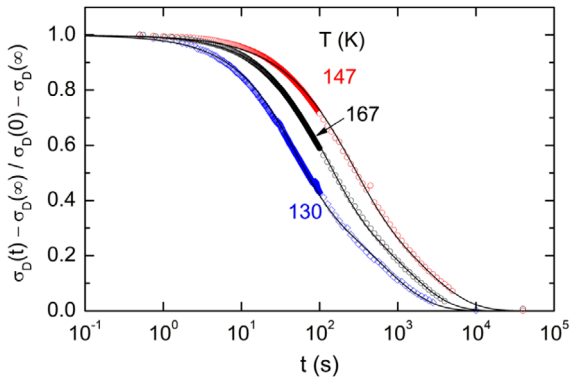

Figure 9. Transients of the normalized dark conductivity of undoped β-Ga_2O_3 at low temperatures. The data are shown by points and the lines are least-squares fits to the sum of two stretched exponential functions.

Similar measurements were performed at low temperatures. The normalized σ_D transients and the corresponding least-squares fits are shown in **Figure 9** by the data points and solid lines, respectively. It is interesting to note that the dark conductivity decreases on a similar time scale compared to the high-temperature decay measurements (Figure 8). This behavior is indicative of a complex microscopic mechanism that involves more than a single metastable state.

Further insight into the governing microscopic mechanism can be obtained from the time constants. **Figure 10** shows the time constants τ_1 and τ_2 as a function of the reciprocal temperature. While the values obtained for τ_1 vary between 45 and 1550 s, a pronounced increase of τ_2 from 550 to 2.9×10^6 s is observed as the temperature increases from 130 to 470 K. Such a behavior of the time constants cannot be explained with a thermally activated process in which charge carriers are released from a metastable state over an energy barrier to a ground state. Rather it indicates that charge carriers are trapped in an energetically broad distribution of localized defects.

Carbon doping of β-Ga_2O_3 causes the dark conductivity transients to become more complex. While for undoped β-Ga_2O_3 two stretched exponentials are sufficient to describe the σ_D

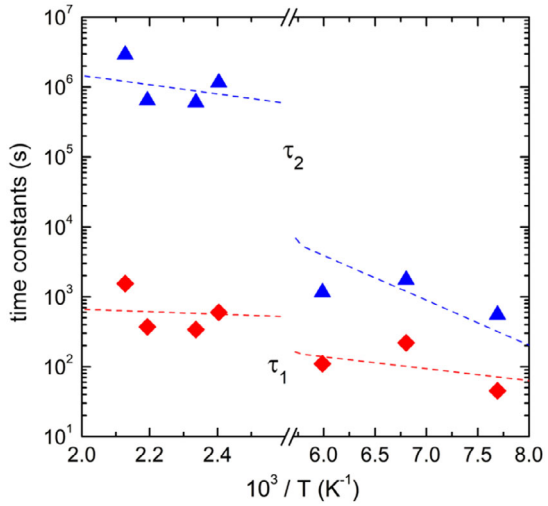

Figure 10. Time constants obtained from fitting the dark conductivity transients plotted in Figure 9 to Equation (1) as a function of the reciprocal temperature.

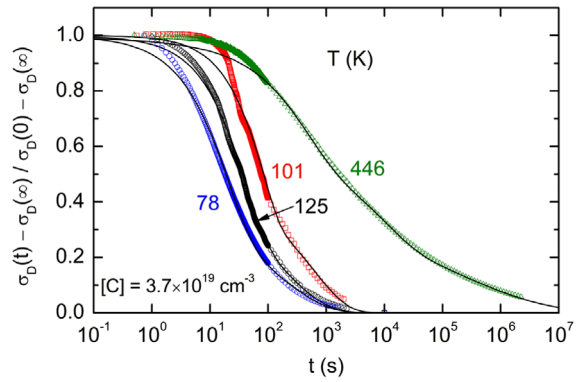

Figure 11. Transients of the normalized dark conductivity of C-doped β-Ga_2O_3. The data are shown by points and the lines are least-squares fits to the sum of three stretched exponential functions.

transients, for C-doped specimens, a third stretched exponential has to be added. Normalized σ_D transients of C-doped β-Ga_2O_3 are shown by the points in **Figure 11**. The data were taken in a temperature range from 78 to 446 K. Similar to undoped β-Ga_2O_3, the conductivity decays more quickly at low temperatures than at high temperatures. This behavior is also supported by the time constants (**Figure 12**). The magnitude of the time constants is also comparable to that of undoped β-Ga_2O_3. However, the need for a third stretched exponential can be explained directly by the introduction of dopants and the accompanying formation of lattice strain.

3.4. Energetic Position of Localized Defects

The relaxation time constants obtained from the dark conductivity decays can be used to estimate the energetic depth of the trapping sites. To leave a localized trap, the charge carriers have to

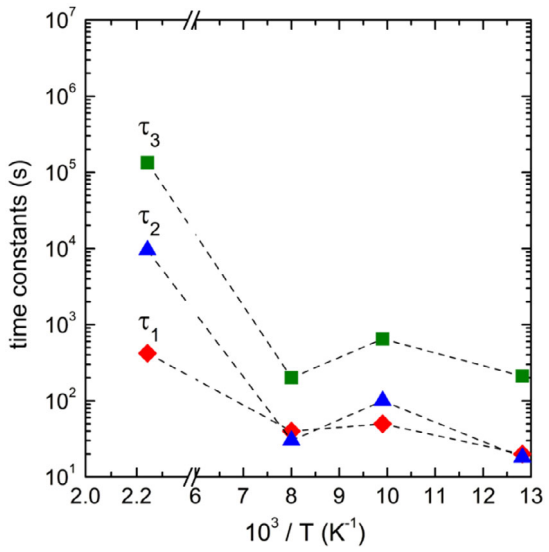

Figure 12. Time constants as a function of the reciprocal temperature. The values were obtained from fitting the dark conductivity transients shown in Figure 11 to three stretched exponential decays.

overcome a potential barrier. This is a thermally activated process, and the time constant is given by

$$\tau = \tau_0 \exp\left(\frac{-E_A}{kT}\right) \tag{2}$$

where $1/\tau_0$ is a phonon frequency, E_A is the activation energy, k is the Boltzmann constant, and T is the temperature. With a prefactor of $\tau_0 = 10^{12}$ s, the activation energies were calculated for each time constant. The energetic positions of the trapping sites with respect to the conduction band edge are plotted in **Figure 13**. At low temperatures the charge carriers have to overcome a barrier of about $E_{CB} - E_T = -0.4$ to -0.5 eV for undoped β-Ga_2O_3.

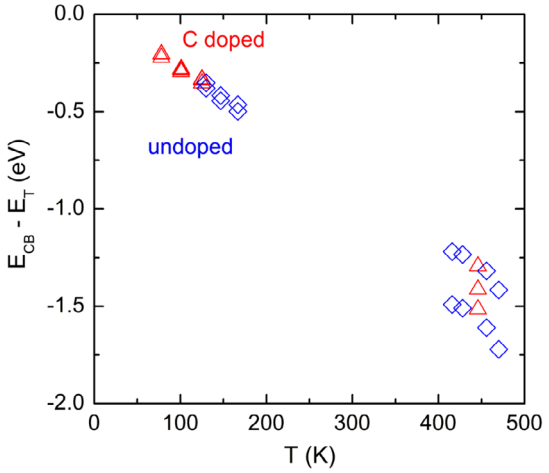

Figure 13. Energy of the localized trapping sites with respect to the conduction band, $E_{CB} - E_T$, as a function of temperature. The triangles and diamonds were obtained from C-doped and undoped β-Ga_2O_3, respectively.

On the other hand, C doping introduces additional shallow traps at $E_{CB} - E_T = -0.2$ to -0.3 eV. The origin of these shallow traps is not due to doping with carbon, since it is a deep donor with an ionization energy of about 0.8 eV.[16] However, the carbon atom with its small atomic radius will introduce strain in the crystal lattice with its nearest neighbor oxygen atoms. Hence, it is conceivable that these strained bonds are the origin of the shallow localized states.

Trapping states at similar energy in the bandgap were reported for Si- and Ge-doped β-Ga_2O_3 grown by molecular beam epitaxy and metal-organic chemical vapor deposition.[21,22] However, localized defect states are not confined to these shallow and deep levels. Ghadi et al.[21] provide an overview of defect states in undoped and doped β-Ga_2O_3 that occur at energies ranging from $E_{CB} - E_T = -0.12$ to -4.4 eV. For most of these defect levels, an assignment to the originating microscopic structure has not yet been made.

At high temperatures, the relaxation measurements sample charge carriers in localized states that are much deeper in energy. For both, undoped and C-doped specimens trapping sites in an energy range of $E_{CB} - E_T = -1.2$ to -1.7 eV are obtained. It is conceivable that these deep traps are due to grain-boundary defects and impurities.

4. Summary

In summary, undoped and C-doped β-Ga_2O_3 thin films were grown by plasma-assisted pulsed laser deposition. The samples are polycrystalline with an average grain size of about 100 nm. Gas phase doping using CO_2 results in C concentrations of maximal 4×10^{19} cm^{-3}, which is low enough that phonon modes are not affected. To investigate charge transport properties, dark conductivity measurements were performed. In the relaxed state A, σ_D changes only very little with temperature for $T < 230$ K, while activated behavior with $E_A = 0.68$ eV is observed for higher temperatures. C doping mainly changes the dark conductivity at elevated temperatures and the activation energy decreases to $E_A = 0.63$ eV. Illumination of the samples with sub-bandgap light results in a pronounced increase of the dark conductivity at low temperatures by up to 6 orders of magnitude. This state B is metastable and an anneal at elevated temperatures restores state A for both undoped and C-doped β-Ga_2O_3. The time and temperature dependence of the relaxation of σ_D was measured. The conductivity transients can be fitted with two or three stretched exponential decays for undoped and C-doped β-Ga_2O_3, respectively. From the time constants, the energetic position of the localized states was estimated. In undoped samples, energies of the traps ranging from $E_{CB} - E_T = -0.4$ to -1.7 eV are obtained. On the other hand, C doping seems to introduce additional shallow states at $E_{CB} - E_T = -0.2$ to -0.3 eV. These shallow states might be caused by strain due to the formation of carbon DX centers.

Acknowledgements

N.M. would like to acknowledge financial support from the Erasmus+ program of the European Union.

Open Access funding enabled and organized by Projekt DEAL.

Conflict of Interest

The authors declare no conflict of interest.

Data Availability Statement

The data that support the findings of this article are available from the authors upon reasonable request.

Keywords

carbon-doped gallium oxides, dark conductivities, metastable states

Received: September 5, 2024
Revised: November 5, 2024
Published online: December 3, 2024

[1] M. Higashiwaki, G. H. Jessen, *Appl. Phys. Lett.* **2018**, *112*, 060401.
[2] M. A. Mastro, A. Kuramata, J. Calkins, J. Kim, F. Ren, S. J. Pearton, *ECS J. Solid State Sci. Technol.* **2017**, *6*, P356.
[3] D. Guo, Z. Wu, P. Li, Y. An, H. Liu, X. Guo, H. Yan, G. Wang, C. Sun, L. Li, W. Tang, *Opt. Mater. Express* **2014**, *4*, 1067.
[4] M. H. Wong, K. Sasaki, A. Kuramata, S. Yamakoshi, M. Higashiwaki, *IEEE Electron Device Lett.* **2016**, *37*, 212.
[5] M. R. Lorenz, J. F. Woods, R. J. Gambino, *J. Phys. Chem. Solids* **1967**, *28*, 403.
[6] J. B. Varley, J. R. Weber, A. Janotti, C. G. Van De Walle, *Appl. Phys. Lett.* **2010**, *97*, 142106.
[7] N. H. Nickel, *Phys. Status Solidi* **2023**, *260*, 2300309.
[8] E. Chikoidze, T. Tchelidze, C. Sartel, Z. Chi, R. Kabouche, I. Madaci, C. Rubio, H. Mohamed, V. Sallet, F. Medjdoub, A. Perez-Tomas, Y. Dumont, *Mater. Today Phys.* **2020**, *15*, 100263.
[9] E. G. Víllora, K. Shimamura, Y. Yoshikawa, T. Ujiie, K. Aoki, *Appl. Phys. Lett.* **2008**, *92*, 202120.
[10] N. Suzuki, S. Ohira, M. Tanaka, T. Sugawara, K. Nakajima, T. Shishido, *Phys. Status Solidi* **2007**, *4*, 2310.
[11] E. Ahmadi, O. S. Koksaldi, S. W. Kaun, Y. Oshima, D. B. Short, U. K. Mishra, J. S. Speck, *Appl. Phys. Express* **2017**, *10*, 041102.
[12] C. Zimmermann, V. Rønning, Y. Kalmann Frodason, V. Bobal, L. Vines, J. B. Varley, *Phys. Rev. Mater.* **2020**, *4*, 074605.
[13] A. T. Neal, S. Mou, S. Rafique, H. Zhao, E. Ahmadi, J. S. Speck, K. T. Stevens, J. D. Blevins, D. B. Thomson, N. Moser, K. D. Chabak, G. H. Jessen, *Appl. Phys. Lett.* **2018**, *113*, 062101.
[14] T. Harwig, J. Schoonman, *J. Solid State Chem.* **1978**, *23*, 205.
[15] M. E. Ingebrigtsen, J. B. Varley, A. Y. Kuznetsov, B. G. Svensson, G. Alfieri, A. Mihaila, U. Badstübner, L. Vines, *Appl. Phys. Lett.* **2018**, *112*, 042104.
[16] S. Lany, *APL Mater.* **2018**, *6*, 046103.
[17] N. F. Mott, *J. Non-Cryst. Solids* **1968**, *1*, 1.
[18] R. M. Hill, *Phys. Status Solidi* **1976**, *34*, 601.
[19] J. Y. W. Seto, *J. Appl. Phys.* **1975**, *46*, 5247.
[20] B. Movaghar, L. Schweitzer, *Phys. Status Solidi* **1977**, *491*, 406.
[21] H. Ghadi, J. F. McGlone, C. M. Jackson, E. Farzana, Z. Feng, A. F. M. A. U. Bhuiyan, H. Zhao, A. R. Arehart, S. A. Ringel, *APL Mater.* **2020**, *8*, 021111.
[22] E. Farzana, E. Ahmadi, J. S. Speck, A. R. Arehart, S. A. Ringel, *J. Appl. Phys.* **2018**, *123*, 161410.